Exact solitary-wave solutions of $\chi^{(2)}$ Ginzburg-Landau equations

Lucian-Cornel Crasovan,[1,2] Boris Malomed,[1,3] Dumitru Mihalache,[2] and Falk Lederer[1]
[1]*Institute of Solid State Theory and Theoretical Optics, Friedrich-Schiller-University Jena, Max-Wien-Platz 1, Jena, D-07743, Germany*
[2]*Department of Theoretical Physics, Institute of Atomic Physics, P.O. Box MG-6, Bucharest, Romania*
[3]*Department of Interdisciplinary Sciences, Faculty of Engineering, Tel Aviv University, Tel Aviv 69978, Israel*
(Received 8 October 1998)

A family of *exact* temporal solitary-wave solutions (dissipative solitons) to the equations governing second-harmonic generation in quadratically nonlinear optical waveguides, in the presence of linear bandwidth-limited gain at the fundamental harmonic and linear loss at the second harmonic, is found, and the existence domain for the solutions is delineated. Direct numerical simulations of the solitons demonstrate that, as well as the classical pulse solutions to the cubic Ginzburg-Landau equation, the dissipative solitons can propagate robustly over a considerable distance before the model's intrinsic instability leads to onset of ''turbulence.'' Two-soliton bound states are also predicted and then found in the direct simulations. We estimate real values of the physical parameters necessary for the existence of the solitons predicted, and conclude that they can be observed experimentally. A promising application for the solitons is their use in closed-loop cavities.
[S1063-651X(99)07306-7]

PACS number(s): 42.81.Dp, 42.65.Ky, 52.35.Sb, 41.20.Jb

I. INTRODUCTION

Much attention has been recently focused on solitons in optical media with the quadratic ($\chi^{(2)}$) nonlinearity, that are supported by the cascading mechanism [1]. Experimental observations of the solitons in the spatial [2] and, very recently, temporal [3] domains were reported. The media in which the solitons exist always have internal losses, which should be compensated by gain. In particular, adiabatic amplification of the spatial solitons was recently analyzed numerically in [4]. However, for the spatial solitons the losses are insignificant in many cases, as the size of the experimental sample is always much smaller than the damping length [2]. Nevertheless, the losses and the gain may be important for temporal solitons circulating in a cavity, where the loss and gain effects will be accumulated as a result of many round trips.

Very recently, temporal solitons in a $\chi^{(2)}$ medium have been experimentally observed for the first time [3]. The solitons were extremely narrow (their temporal width was 58 fs), which allowed to observe them in a small sample (7 mm long) of the $\chi^{(2)}$ optical crystal (the so-called BBO). The use of those solitons in applications, such as all-optical switching and others, would require to place the crystal into a cavity (e.g., a ring resonator). For so temporally narrow solitons circulating in the cavity, the *filtering* losses will be especially important. Thus, both the losses and amplification must be taken into consideration.

The action of pure losses on the $\chi^{(2)}$ solitons was considered in some works (see, e.g., [5]). The objective of this work is to introduce a $\chi^{(2)}$ model including the losses *and* compensating gain, i.e., essentially, $\chi^{(2)}$ *Ginzburg-Landau equations*, and to find their *exact* solitonlike solutions. In fact, these solutions combine two classical solitary-pulse solutions: the Karamzin-Sukhorukov soliton in the lossless $\chi^{(2)}$ medium [6], and the Pereira-Stenflo [7] (see also [8]) dissipative soliton in the cubic complex Ginzburg-Landau (CCGL) equation. The model is introduced, and its special exact soliton solutions are obtained, in Sec. II. Obviously, a crucially important issue is the stability of these solitons. Results of the direct numerical simulations of the solitons' stability are collected in Sec. III. We arrive at a conclusion that the solitons are subject to the obvious background instability, which is a common feature of the Ginzburg-Landau equations including the linear gain term, but, nevertheless, they are meaningful objects, as they can robustly propagate over ~ 10 soliton's dispersion lengths, which is quite sufficient for their formation and observation. Additionally, in Sec. III we display two-soliton bound states, which can be easily predicted and found in the simulations. In the same section, we also give estimates for the necessary values of the physical parameters (such as the size of the crystal sample and the gain strength and bandwidth), referring to experimental data reported in [3]. The results of the work are briefly summarized in Sec. IV.

II. MODEL AND EXACT SOLITON SOLUTIONS

Because the model must include two equations, one for the fundamental harmonic (FH) and the other for the second harmonic (SH), it is necessary to understand at what place the losses and amplification should be included. As for the losses, it is very natural to assume that the losses at SH are dominating, while those at FH are negligible (note that the most fundamental contribution to the losses, the Rayleigh scattering, has its intensity growing with the frequency ω as ω^4). On the other hand, the amplifier should operate at FH, as, otherwise, the amplification will not be efficient (in real solitons, the SH component is always weaker than the FH one, and it is natural to apply the gain to the stronger component). So, we will adopt a model combining losses at SH and bandwidth-limited gain at FH.

The solitons that we will find (as well as the well-known CCGL dissipative solitons) are subject to the usual background instability, which is an inherent feature of the model containing linear gain; however, it will be shown that the solitons can travel a reasonably long distance (several their

own *dispersion lengths*) before the onset of the instability. Moreover, the instability may be immaterial in a real physical situation, provided that the propagation distance necessary for the instability onset is larger than the actual size of the system. The latter circumstance is especially important for the closed-loop cavities: if the length of the instability-generating part of the loop is not too long, *stable* multisoliton patterns are possible in it, with regard to the periodic boundary conditions in the propagation coordinate Z [9].

Our model is based on the propagation equations for the FH and SH waves with the local amplitudes A and B:

$$\begin{aligned} iA_Z + icA_T - (1/2)DA_{TT} + A^*B &= i\gamma_0 A + i\gamma_1 A_{TT}, \\ iB_Z - (1/2)\sigma DB_{TT} - \beta B + 2A^2 &= -i\Gamma_0 B + i\Gamma_{1/2} B_T + i\Gamma_1 B_{TT}, \end{aligned} \tag{1}$$

where T and D are, as usual, the reduced time and chromatic-dispersion coefficient, σ is the *relative* SH dispersion coefficient, β and c are the phase- and group-velocity mismatches, γ_0 is the FH gain coefficient, γ_1 accounts for the finite size of the gain band (γ_1 can be enhanced, if necessary, by means of inserted optical filters), while Γ_0, $\Gamma_{1/2}$, and Γ_1 control the losses at SH. The FH equation in system (1) implies that the carrier frequency is chosen as that at which the gain has a maximum (that is why an extra term $i\gamma_{1/2}A_T$, similar to the one $i\Gamma_{1/2}B_T$ in the SH equation, is absent; as for the coefficient $\Gamma_{1/2}$, it vanishes only in the special case when the SH losses have a minimum at the frequency which is exactly twice that at which the FH gain has its maximum). The group-velocity mismatch c can be eliminated by an obvious transformation in the conservative version of the model, but not in the one including the losses and gain. The parameters D, σ, c, β, and $\Gamma_{1/2}$ may have any sign, while all the other parameters on the right-hand sides of the equations are positive (Γ_0 may, also, be zero; see below).

The model (1) is too complicated to seek for its exact solitary-wave solutions. However, we note that the group-velocity mismatch is negligible if $|c| \ll |D|(\Delta\omega)^2$, $\Delta\omega$ being the spectral width of the pulse to be dealt with. As it will be seen below, the real temporal $\chi^{(2)}$ solitons [3] have a fairly large bandwidth, $\Delta\omega \sim 10$ THz, and propagate at a strong anomalous FH dispersion, $D \sim -1$ ps^2/m, which gives rise to $|D|(\Delta\omega)^2 \sim 10^{-11}$ s/m. Consequently, any group-velocity difference essentially smaller than ~ 500 km/s is negligible, and, in view of this, we set $c=0$ in what follows below. Also, due to the large value $\Delta\omega \sim 10$ THz, we may take $\Gamma_{1/2}=0$, as the slope $\Gamma_{1/2}$ of the SH losses may be neglected if the shift of the SH carrier frequency from the minimum-loss point is much smaller than $\Delta\omega$. Lastly, using the obvious scale invariance of the equations, we set $D \equiv -1$ (assuming anomalous dispersion at FH, which is the case in the real situation [3]), and $\gamma_0 \equiv 1$. Thus, we will deal with a simplified version of the underlying model (1),

$$\begin{aligned} iA_Z + (1/2)A_{TT} + A^*B &= iA + i\gamma_1 A_{TT}, \\ iB_Z + (1/2)\sigma B_{TT} - \beta B + 2A^2 &= -i\Gamma_0 B + i\Gamma_1 B_{TT}. \end{aligned} \tag{2}$$

Following the works [6] and [7], we look for solitary-pulse solutions to Eqs. (2) in the form

$$\begin{aligned} A &= a[\mathrm{sech}(\lambda T)]^{2+i\mu} e^{ikZ}, \\ B &= b[\mathrm{sech}(\lambda T)]^{2+2i\mu} e^{2ikZ}, \end{aligned} \tag{3}$$

where a and b are the FH and SH amplitudes, λ is the inverse width of the pulse, μ is its *chirp*, and k is the FH wavenumber. The latter three parameters are always real, while the amplitudes a and b may be complex. However, a can be made real by means of a trivial phase shift, therefore the only complex unknown is b.

Substituting the above ansatz into Eqs. (1), we arrive at an overdetermined system of four complex equations for the four real and one complex unknowns, λ, μ, k, a, and b. Obviously, a solution may be possible if two constraints are imposed on the five real parameters σ, β, γ_1, and $\Gamma_{0,1}$ of model (2). This still leaves us with three free parameters, leading to a very involved analysis.

In order to present the results in a clearer form, we will first dwell on the particular case $\Gamma_0=0$, implying exact compensation of the SH loss at its minimum, which is quite easy to realize physically. In this case, we obtain, from the above-mentioned equations (not displayed here), two values of μ,

$$\mu_\pm = (1/2)(-\alpha \pm \sqrt{\alpha^2+4}), \tag{4}$$

where $\alpha \equiv \sigma/\Gamma_1$. For either value of μ, we find the corresponding values of λ, k, a, and b. Additionally, in accord with what was said above, we need to impose two constraints on the model's parameters, which we choose in a form that determines γ_1 and β as functions of the remaining free parameters, σ and Γ_1. Defining $t_1 \equiv 90\mu - 30\mu^3$ and $t_2 \equiv 36 - 80\mu^2 + 4\mu^4$, we can cast the results into the form

$$\lambda = (-4\gamma_1 + 2\mu + \gamma_1\mu^2)^{-1/2}, \quad k = \frac{1}{2}\lambda^2(4 + 8\gamma_1\mu - \mu^2),$$

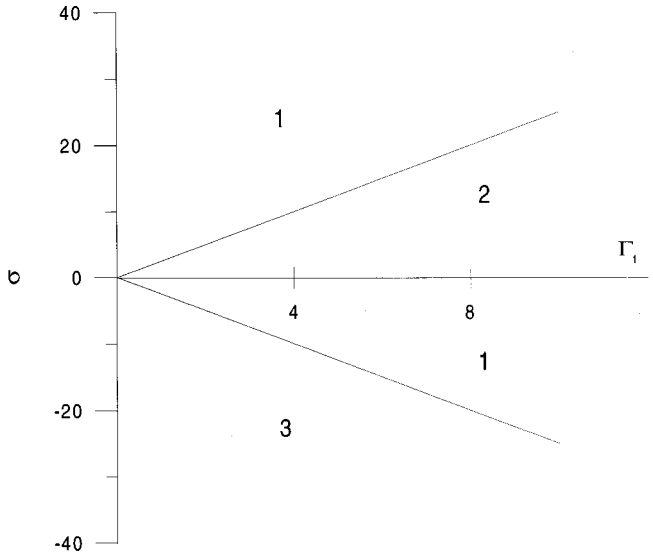

FIG. 1. Existence domain of the solitary-pulse solutions in the particular case $\Gamma_0=0$. In the regions labeled 1, 2, and 3, there exist, respectively, two solutions corresponding to $\mu_\pm$ in Eq. (4), the single solution corresponding to μ_+, and the single solution corresponding to μ_-.

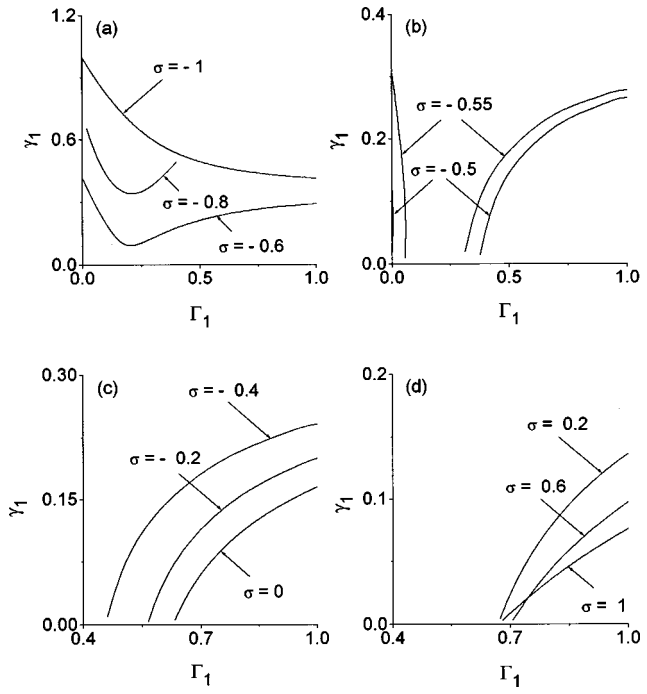

FIG. 2. Existence curves for the exact solitary pulse in the case $\Gamma_0=1$. Shown is the solution with the positive root μ_+ in Eq. (8).

$$b=\lambda^2\left(\frac{1}{2}-i\gamma_1\right)(2+i\mu)(3+i\mu),$$

$$a=(\lambda/2)\sqrt{(\sigma-2\Gamma_1)(2+2i\mu)(3+2i\mu)b}, \tag{5}$$

$$\gamma_1=\frac{1}{2}\,\frac{\alpha t_1-2t_2}{2t_1+\alpha t_2},\quad \beta=-2k+2\Gamma_1\lambda^2(\alpha+4\mu-\alpha\mu^2). \tag{6}$$

The parametric constraints (6) secure the reality of the expression under the square root in the solution (5) for a. Additionally, it is necessary to have this expression, as well as that under the square root for λ, positive, as both a and λ must be real. This gives rise to inequalities

$$-4\gamma_1+2\mu+\gamma_1\mu^2>0,\quad t_1(\Gamma_1+\sigma\gamma_1)>0, \tag{7}$$

which determine the existence domain of the *exact* solutions in the plane of the remaining free parameters (σ,Γ_1). The domain is shown in Fig. 1.

To present the results at $\Gamma_0\neq 0$, we choose $\Gamma_0=1$. In this case, the expression for μ is more cumbersome than Eq. (4):

$$\mu_\pm=\frac{-(2\sigma+1)\pm\sqrt{(2\sigma+1)^2+4(4\Gamma_1+\gamma_1)(\Gamma_1+\gamma_1)}}{(4\Gamma_1+\gamma_1)}. \tag{8}$$

Using the same notation as above, we can cast the solution into the form (5) which is supplemented by the parametric constraints,

$$\beta=-2k+2\lambda^2(\sigma+4\mu\Gamma_1-\sigma\mu^2),$$
$$(\sigma/4-\Gamma_1\gamma_1)t_1-(\Gamma_1+\sigma\gamma_1)t_2/2=0, \tag{9}$$

and by the inequalities (7).

The second relation in Eq. (9) allows us to choose two free parameters out of σ, Γ_1, and γ_1. Fixing σ, we thus represent the constraint in the form $\gamma_1=\gamma_1(\Gamma_1)$. Adding then the inequalities (7), we can completely determine the existence domain. Figure 2 shows the curves $\gamma_1(\Gamma_1)$ on which the solution exists for some representative values of σ. The value $\sigma=-0.5$ is a critical one, at which the shape of the curves changes.

III. NUMERICAL SIMULATIONS OF THE SOLITONS' STABILITY AND THE ESTIMATE OF THE PHYSICAL PARAMETERS

We have numerically checked the stability of the exact solitary pulses found in the analytical form in the preceding section. Simulating the full system of Eqs. (2), we have seen (as one should expect) that they finally develop the background instability, but only after a considerable propagation distance, see a typical example in Fig. 3. In the case shown in Fig. 3, for instance, the robust stage of propagation extends to ≈ 10 dispersion lengths, which is quite sufficient for experimental observation of the pulses.

To estimate the values of the physical parameters corresponding to the situation displayed in Fig. 3, we take the values of the dispersion at which the temporal $\chi^{(2)}$ soliton was observed in Ref. [3], which is $D\sim -1$ ps^2/m, and the temporal width of the soliton, 58 fs, from the same work, yielding the dispersion length $z_D\sim 3$ mm (note that this com-

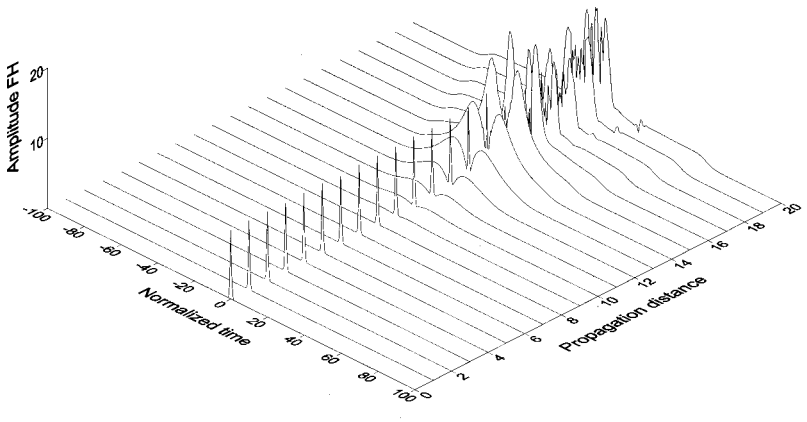

FIG. 3. Numerically simulated propagation of the solitary pulse at the values of the parameters: $\gamma_0=1$, $\gamma_1=0.06044$, $\Gamma_0=0$, $\Gamma_1=0.25$, $\sigma=1$, and $\beta=-7.26296$. In this case we have $a=9.87120$, $\lambda=2.06834$, and $\mu_+=0.23607$. Only the evolution of $|A|$ is shown here.

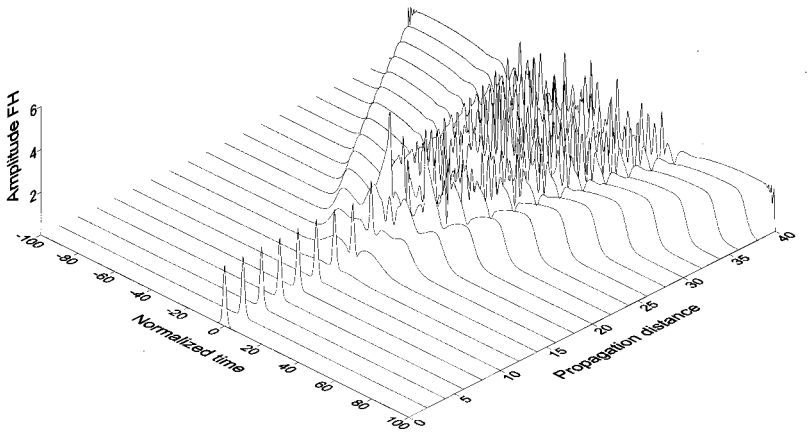

FIG. 4. Same as in Fig. 3 for the values of the parameters $\gamma_0=1$, $\gamma_1=0.10824$, $\Gamma_0=1$, $\Gamma_1=0.8$, $\sigma=0$, and $\beta=0.81291$. In this case, the solution has $a=2.833\,78$, $\lambda=0.908\,69$, and $\mu_+=0.788\,38$.

plies with the length 7 mm of the sample used in the experiment). The values of the dimensionless parameters given in the caption to Fig. 3 then imply that the necessary gain is

$$\gamma_0 \sim (4z_D)^{-1} \sim 0.1 \ \text{mm}^{-1}, \tag{10}$$

and the filtering strength is

$$\gamma_1 \sim 50\,\text{ps}^2/\text{km}, \quad \Gamma_1 \sim 250 \ \text{ps}^2/\text{km} \tag{11}$$

for FH and SH, respectively.

In a real experiment, two different setups are possible: (i) a lumped one, in which the $\chi^{(2)}$ crystal, the amplifier, and the filters (if they are necessary) are separately included into the closed-loop cavity, and (ii) an integrated setup, in which the $\chi^{(2)}$ crystal is doped by resonant atoms and optically pumped by an external source, so that the crystal is, simultaneously, the distributed amplifier. Then, the integrated unit is inserted into the cavity. Model (2) qualitatively correctly describes the setups of both types, but the above exact solutions directly apply only to the integrated setup. An additional advantage of the latter case is that the resonant dopant also provides for enhanced dispersion at FH, which would allow one to use optical pulses that are not so narrow.

In the integrated setup, the value (10) of the gain, although being high (~ 500 times the gain in the usual Erbium-doped fiber amplifier [10], that, however, operates at a different wavelength), is quite achievable (the minimum possible length of the active region providing for the necessary amplification is ~ 0.2 mm, which is much smaller than the relevant lengths). Note that, in the integrated scheme, no added filters are present, but filtering is provided by the natural gain bandwidth Ω. The characteristic values (10) and (11) yield an estimate $\Omega \sim 10$ THz. This value of the bandwidth is not something impossible, as, e.g., the above-mentioned Erbium-doped amplifiers have the bandwidth of the same order of magnitude [10]. It is relevant to stress that the 58-fs-wide soliton generated in the work [3] has its bandwidth $\Delta\omega$ also ~ 10 THz, so that the necessary values prove to be self-consistent.

Last, the size of the crystal sample large enough to observe the solitons but not too large, so that to prevent the onset of the background instability, is, according to the above numerical results, $\lesssim 10 z_D$, i.e., $\lesssim 30$ mm, which is quite realistic. Such an experimental setup should make it feasible to observe the predicted solitons experimentally. If included into a closed cavity, it may readily provide for stable circulation of the soliton, which opens way to various practical applications. It is also relevant to stress that a simpler scheme mentioned above, with the lumped $\chi^{(2)}$ crystal, amplifier, and filters, even though it is not exactly described by the above model, may provide for very similar, but easier-to-achieve, physical results.

We have also performed the simulations of Eqs. (2) with the initial conditions taken as the solitary pulse given by Eqs. (5), (8), and (9), corresponding to $\Gamma_0 \neq 0$. Figure 4 demonstrates, for this case, eventual onset of the instability similar to that found in the previous case (Fig. 3), i.e., after the propagation of the soliton over ≈ 10 dispersion lengths.

As is well known, the linear dissipation and gain terms make the soliton's tails oscillating, which gives rise to two-soliton and multisoliton bound states (see Ref. [11] and references therein). We have simulated this case too, and indeed observed bound states of two pulses that exist over a finite propagation distance before the onset of the instability. A typical example of the two-soliton bound state is displayed in Fig. 5.

IV. CONCLUSION

In this work, we have proposed $\chi^{(2)}$ Ginzburg-Landau equations and found particular exact solitary-pulse solutions to them. Direct simulations demonstrate that, depending on the parameters, the pulses are robust over a sufficiently long propagation distance before the onset of instability, which may allow experimental observation of the pulses, e.g., in cavities, and also has a potential for applications. Bound

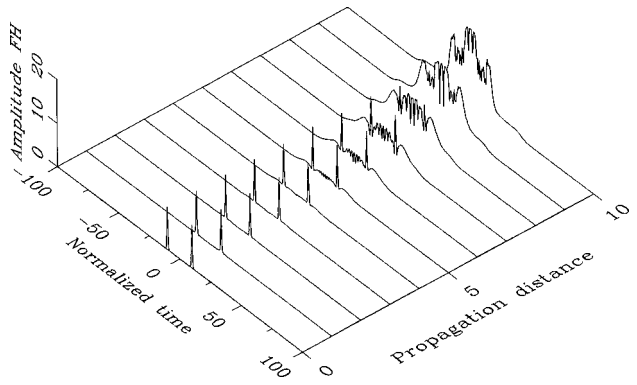

FIG. 5. Typical example of a bound state of two pulses. The parameters are as in Fig. 3.

states of two pulses were also predicted and found in the simulations. An estimate, using the recently published experimental data, shows that the values of the physical parameters necessary for the observation of the predicted soliton are quite realistic.

It is relevant to note that the pumped waveguide can be stabilized by linearly coupling it (placing parallel) to an auxiliary dissipative waveguide, in combination with the filters. As it was shown in [12] in terms of the cubic Ginzburg-Landau equation, this opens the way to have *completely stable* localized pulses. The corresponding modification of the present model has indeed produced stable pumped $\chi^{(2)}$ solitons. These results will be presented in detail elsewhere.

ACKNOWLEDGMENTS

We appreciate valuable discussions with L. Torner and D. Mazilu. L.-C.C. acknowledges the DAAD for supporting his stay at Friedrich-Schiller-Universität Jena, and B.A.M. appreciates a support from the Institute of Solid State Theory and Theoretical Optics at the Friedrich-Schiller-Universität Jena.

[1] G.I. Stegeman, D.J. Hagan, and L. Torner, Opt. Quantum Electron. **28**, 1691 (1996).

[2] W. E. Torruellas, Z. Wang, D.J. Hagan, E. W. Van Stryland, G.I. Stegeman, L. Torner, and C.R. Menyuk, Phys. Rev. Lett. **74**, 5036 (1995); R. Schiek, Y. Baek, and G.I. Stegeman, Phys. Rev. E **53**, 1138 (1996).

[3] P. DiTrapani, D. Caironi, G. Valiulis, A. Dubietis, R. Danielius, and A. Piskarskas, Phys. Rev. Lett. **81**, 570 (1998).

[4] L. Torner, Opt. Commun. **154**, 59 (1998).

[5] L. Torner, D. Mihalache, D. Mazilu, and N.N. Akhmediev, Opt. Lett. **20**, 2183 (1995); B.A. Malomed, D. Anderson, M. Florjanczyk, and M. Lisak, Pure Appl. Opt. **5**, 941 (1996).

[6] Yu.N. Karamzin and A.P. Sukhorukov, Pis'ma Zh. Éksp. Teor. Fiz. **20**, 734 (1974) [JETP Lett. **20**, 339 (1974)]; Zh. Éksp. Teor. Fiz. **68**, 834 (1975) [Sov. Phys. JETP **41**, 414 (1976)].

[7] N.R. Pereira and L. Stenflo, Phys. Fluids **20**, 1733 (1977).

[8] L.M. Hocking and K. Stewartson, Proc. R. Soc. London, Ser. A **326**, 289 (1972).

[9] B.A. Malomed, A. Schwache, and F. Mitschke, Fiber Integr. Opt. **17**, 267 (1998).

[10] E. Desurvire, *Erbium-Doped Fiber Amplifiers* (Wiley & Sons, New York, 1994).

[11] V.V. Afanasjev, B.A. Malomed, and P.L. Chu, Phys. Rev. E **56**, 6020 (1997).

[12] B.A. Malomed and H.G. Winful, Phys. Rev. E **53**, 5365 (1996); J. Atai and B.A. Malomed, *ibid.* **54**, 4371 (1996).